**Author**: Flach, K.D.
**Title**: Holding the balance; the equilibrium between ERα-activation, epigenetic alterations and chromatin integrity
**Issue Date**: 2018-09-25

# Chapter 2

## *Posttranslational modification of ERα -part 1*

*Adapted from Oncogene, De Leeuw et al., 2013*

**PKA phosphorylation redirects ERα to promoters of a unique gene set to induce tamoxifen resistance**

R de Leeuw[1], KD Flach[2], C Bentin Toaldo[1], X Alexi[2], S Canisius[2,3], J Neefjes[1], R Michalides[1] and W Zwart[2]

[1]Department of Cell Biology, The Netherlands Cancer Institute, Amsterdam, The Netherlands
[2]Department of Molecular Pathology, The Netherlands Cancer Institute, Amsterdam, The Netherlands
[3]Department of Molecular Biology, The Netherlands Cancer Institute, Amsterdam, The Netherlands
*Oncogene (2013) 32, 3543–3551*

**Abstract**

Protein Kinase A-induced estrogen receptor alpha (ERα) phosphorylation at serine residue 305 (ERαS305-P) can induce tamoxifen resistance in breast cancer. How this phospho-modification affects ERα specificity and translates into tamoxifen resistance is unclear. Here we show that S305-P modification of ERα reprograms the receptor, redirecting it to new transcriptional start sites, thus modulating the transcriptome. By altering the chromatin-binding pattern, Ser305 phosphorylation of ERα translates into a 26-gene expression classifier that identifies breast cancer patients with a poor disease outcome after tamoxifen treatment. MYC-target genes and networks were significantly enriched in this gene classifier that includes a number of selective targets for ERαS305-P. The enhanced expression of MYC increased cell proliferation in the presence of tamoxifen. We demonstrate that activation of the PKA signaling pathway alters the transcriptome by redirecting ERα to new transcriptional start sites, resulting in altered transcription and tamoxifen resistance.

**Introduction**

Breast cancer is the most frequently diagnosed malignancy among women, with annually around 1.7 million new diagnoses worldwide. Although treatment has strongly improved with the development of adjuvant systemic therapies, still about half a million patients die of the consequences of breast cancer every year (1). The choice of adjuvant treatment is largely based on the pathological subtype of the breast tumor, which can be classified by morphological, molecular and immunohistochemical markers. These subtypes correspond to distinct transcriptional repertoires, which translates in different aggressiveness and metastatic potential (2). 75% of all breast tumors are luminal and proliferation is dependent on the activity the estrogen receptor α (ERα). Inhibition of ERα by endocrine therapy is therefore a major treatment modality for these tumors. Endocrine therapy can be subdivided into two treatment modalities; aromatase inhibitors that block synthesis of the hormone estrogen and anti-estrogens. Anti-estrogens (e.g. tamoxifen) compete with natural estrogens by occupying the hormone-binding site of ERα and either arrest it in the inactive state (3) or inducing degradation of the receptor (4). However, patients can acquire resistance to either type of endocrine therapy. About 25% of the tamoxifen-treated tumors are resistant to this anti-estrogen, even though the tumor continues expressing ERα (5). Consequently, patients unresponsive to tamoxifen may still respond to other anti-estrogens such as fulvestrant or to aromatase inhibitors (4). A major step in treatment success would be achieved when responses to endocrine treatment could be predicted on an individualized basis. Detection of ERαS305-P in patient tissues has enabled the identification of subsets of patients resistant to tamoxifen prior to the onset of treatment (6,5,7). However, not all tamoxifen-resistant patients can be identified by IHC staining, and alternative resistance-inducing mechanisms are likely to play a role in the remaining patient group. Indeed, several causes and contributing factors in tamoxifen resistance have been described in breast cancer patients or cell models, including upregulation of growth factor receptors (like EGFR (8,9), IGFR and HER2 (10,11)), activation of kinases (such as AKT (12), MAPK (13,14), PKA in combination with PAK1 (6,15,16)), and resulting phosphorylation status of ERα (17,18,19,20).

The effects of PKA-induced phosphorylation of ERα at Serine residue 305 (ERαS305-P) in the region between the ligand binding domain and the DNA binding domain are understood in molecular detail. Phosphorylation at Ser305 results in a conformational arrest when exposed to tamoxifen (17), which affects recruitment of coregulators (21). Consequently, tamoxifen acts as an agonist of ERα instead of an antagonist, now inducing cell growth of breast cancer cell lines (17,22). An antibody detecting ERαS305-P in tumor sections was successful in identifying breast cancer patients with a poor outcome after tamoxifen treatment (6,5,7), translating observations in tissue culture into clinical patient responses.

Since ERα is a nuclear receptor, and its phosphorylation affects recruitment of coregulators, the chromatin binding landscape of ERα and corresponding influence on the transcriptome may change due to this modification. Several kinase pathways including PKA are linked to tamoxifen resistance (22,17,23). Several classical targets for ERα were differentially regulated by PKA, including TFF1 (22). PKA activation does not only phosphorylate ERα, but has many targets, including coregulators of the receptor (24,25,26). The phospho-status of coregulators can also affect ERα function, thereby indirectly affecting the ERα cistrome and transcriptome (26,27). Other PKA targets may even bypass the receptor and change the transcriptome independently. Since kinase activity can alter the chromatin-interaction landscape of ERα (28), deciphering a direct connection between ERαS305-P modification and its targets is essential for understanding tamoxifen resistance. Here, we aim to define the direct target genes of ERαS305-P and test whether this yields predictors for tamoxifen resistance. We determined the resulting transcriptome and performed further bioinformatic analyses to determine a predictive gene signature in patient material. This signature includes unique ERαS305-P induced pathways that explain PKA-related tamoxifen resistance.

## Results

### ERαS305 phosphorylation by Protein Kinase A

To study PKA-induced tamoxifen resistance, we used two well-defined and intensely studied breast cancer cell lines MCF7 and MDA-MB134. Both MCF7 and MDA-MB134 express ERα and require estrogens for growth, which is inhibited by tamoxifen (17,29). In MCF7 cells, we activated the PKA pathway by forskolin (30) (**Figure 1A** top) and isolated RNA for microarray and qPCR analyses after 4 hours of tamoxifen exposure to probe early transcriptional responses of ERαS305 phosphorylation. Forskolin treatment induces phosphorylation of ERαS305 as detected by a specific antibody (**Figure 1B** top). While we chemically activated the PKA pathway in MCF7 cells, we decided to confirm results by genetically activating this pathway in MDA-MB134 cells. Here, PKA was activated by silencing the inhibitory

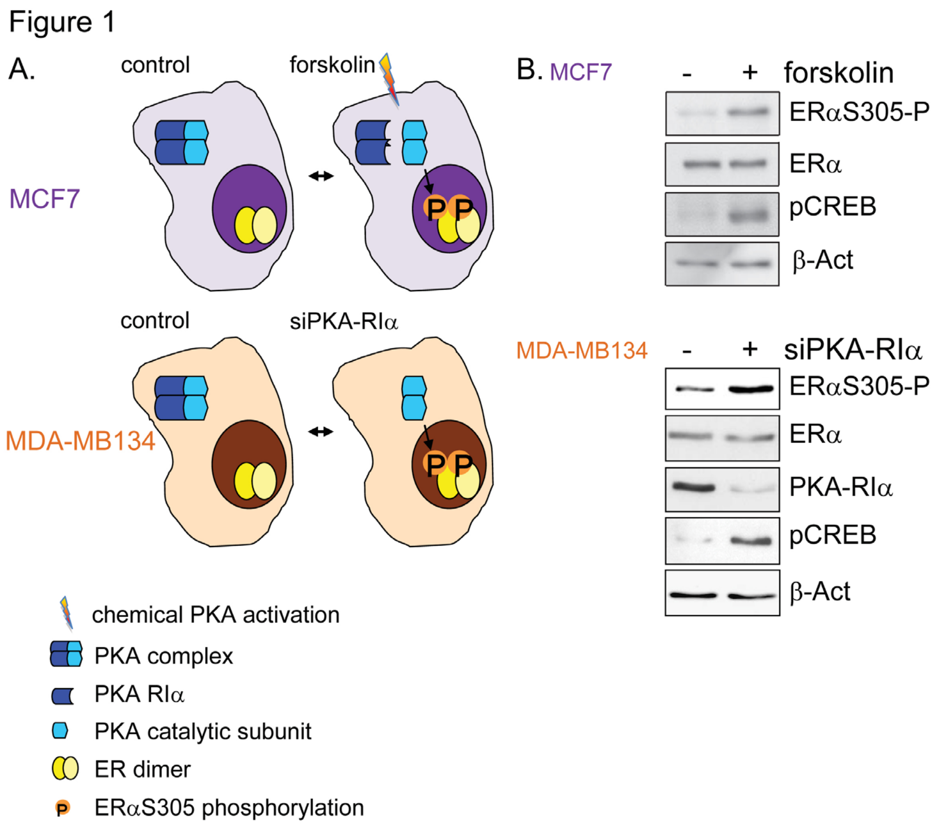


**Figure 1:** *ERαS305 phosphorylation by Protein Kinase A.*
*(A) Experimental setup to activate PKA in MCF7 (top) by forskolin stimulation and in MDA-MB134 (bottom) by PKA-RIα knockdown with lentiviral shRNA. Dissociation (MCF7) or loss (MDA-MB134) of PKA-RIα liberates the active, catalytic subunit of PKA, leading to ERαS305 phosphorylation. (B) Western blot analysis of the model systems. Top: Forskolin treatment of MCF7 cells leads to activated PKA, illustrated by increased p-CREB, and elevated ERαS305 phosphorylation. Bottom: shRNA approach successfully decreases PKA-RIα level in MDA-MB134 cells, leading to increased p-CREB and ERαS305-P.*

subunit of PKA, PKA-RIα (**Figure 1A** bottom) (31), which is also observed in tamoxifen-resistant patients (17). When PKA-RIα is silenced, PKA is activated yielding phosphorylation of ERαS305 (17), which was confirmed by Western blot analysis (**Figure 1B** bottom). In addition, increased phosphorylation of PKA substrate CREB confirms that PKA is activated in both cell lines (**Figure 1B**), yielding an elevated ERαS305-P signal. When both methods of

PKA activation were exchanged between the two cell lines, this still resulted in ERαS305 phosphorylation (**Suppl. Figure S1**).

**A gene signature for tamoxifen resistance after PKA activation**

We analysed the effects of PKA-induced ERαS305 phosphorylation on the transcriptome by expression microarray analysis. Under conditions corresponding to the experiments above (**Figure 1**), cells were deprived of hormones for three days and subsequently treated with tamoxifen, after which the influence of PKA activation was assessed in both cell lines (**Figure 2**). Gene expression distribution is illustrated by the log-ratio, for PKA-activated versus non-activated cells, over intensity (RI) dot plots (**Figure 2A**). In MCF7 cells, we identified 152 upregulated and 108 downregulated genes following PKA activation (260 in total). In MDA-MB134, we found 385 up- and 437 downregulated genes (822 in total) (**Supplementary Table S1 and S2**). In these gene expression profiles, 59 up- and 41 downregulated genes overlapped between MCF7 and MDA-MB134 cells (**Figure 2B and Suppl. Table S3 and S4**). By focusing on the overlap of 100 differentially regulated genes, we eliminated cell line or treatment-specific effects. Among the upregulated hits were two classical ERα gene targets: XBP1 and TFF1, the latter of which was in the top 5 of differentially regulated genes. The top 10 up- and downregulated hits for MCF7 and MDA-MB134 cells are indicated (**Figure 2C**), and a subset was tested and confirmed by qPCR (**Figure 2D**). Next, we tested the 100 differentially regulated genes that are shared between the two cell lines and conditions (59 up, 41 down) as a classifier for outcome in tamoxifen treated breast cancer patients, using a publically available dataset (32). The gene classifier was found to significantly correlate with poor outcome after tamoxifen treatment ($p=0.019$; hazard ratio=2.5) (**Figure 2E** top). This classifier was validated in an independent patient series (33), again identifying the patients with a poor outcome after tamoxifen treatment ($p=0.045$; hazard ratio=1.97, **Figure 2E** bottom).

Figure 2

A. RI plots

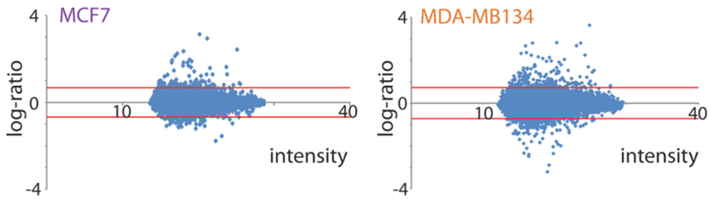


B.

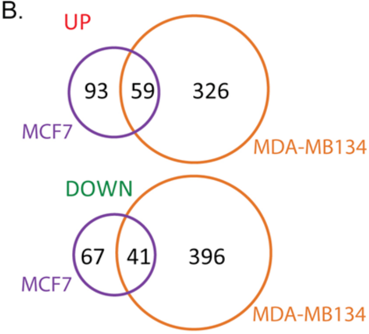


C.

**Top 10 hits**

| MCF7* | | MDA-MB134* | |
|---|---|---|---|
| UP | DOWN | UP | DOWN |
| ASS | CLIC3 | CPE | CAV1 |
| TFF1 | AHNAK | TFF1 | CAV2 |
| MUC5AC | CAV1 | ADORA1 | SAMD11 |
| ADORA1 | TACC1 | SLC7A5 | KLHL24 |
| SLC7A5 | PMP22 | PRSS23 | CLIC3 |
| ISG20 | RAMP3 | SLC7A2 | CXCR7 |
| CPE | YPEL3 | IER3 | SCUBE2 |
| PCP4 | NRCAM | ASS | SMAD3 |
| SEMA3B | GPER | SEMA3B | TSPAN9 |
| IER3 | SMAD3 | HS.579631 | TACC1 |

* all hits overlap between MCF7 and MDA134

D. qPCR

E.

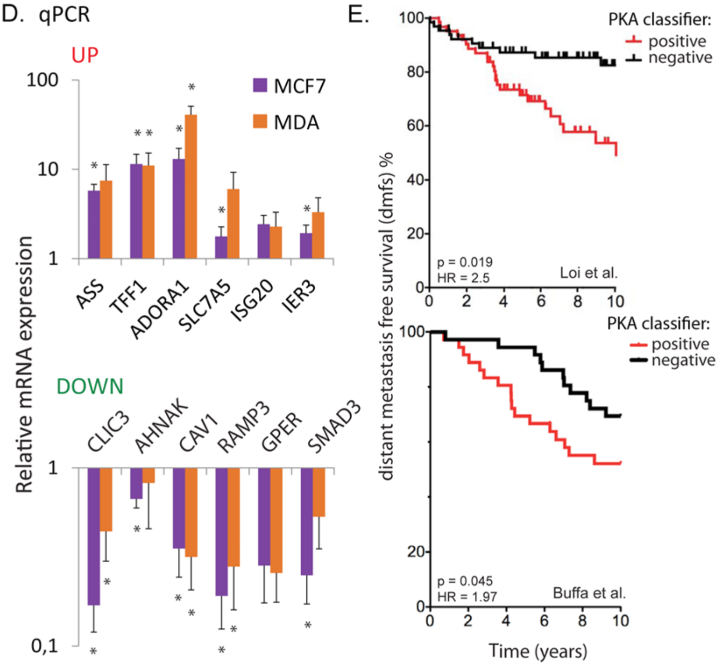

**Figure 2**: *Gene signature for tamoxifen resistance through PKA activation (A) RI-plots of microarray profiles of MCF7 (left) and MDA-MB134 (right). Log-ratio is plotted over intensity. For further analysis, a threshold is used of >1.5x difference (log-ratio = 0.585), indicated by the red line, and p<0.05. (B) Venn diagrams of up- (top) and downregulated (bottom) genes show overlap between MCF7 (purple) and MDA-MB134 (orange) gene expression signatures.(C) Table of the top 10 of up- and downregulated genes for MCF7 and MDA-MB134 mRNA expression values. Genes represented in red (up) or green (down) are tested and confirmed by qPCR. (D) qPCR validation of a subset of the top hits. mRNA expression is shown as a ratio tamoxifen/tamoxifen with PKA activation, and internally corrected using β-Actin. MA = Microarrays values. Error bars represent standard error of the mean (SEM). * p < 0.05 by Student's t-test. (E) Genes shared between MCF7 and MDA-MB134 are combined into a 100-gene signature. This signature was applied as a gene classifier in a disease metastasis free survival analysis. The average gene expression values in ERα positive, endocrine treated patients selected from Loi et al. (top, (32)) and Buffa et al. (bottom, (33)) were calculated and ranked for up- and downregulated genes. Patients were stratified as described in the materials and methods. Patients who have a positive signature for the classifier show significantly worse disease progression (Loi data: p=0.019; hazard ratio(HR)=2.5; Buffa data: p=0.045; HR=1.97)*

**S305P modification of ERα targets the receptor to promoters**

PKA activity results in the phosphorylation of many targets, including ERα. ERα itself has two target sites for PKA, Serine 236 (34) and Serine 305, the latter of which is predominant and correlates to tamoxifen resistance (17). To determine the effects of ERαS305 phosphorylation on gene transcription and chromatin deposition, we analyzed the chromatin-binding landscape of ERαS305-P by means of ChIP-seq with a specific monoclonal antibody (5). To this purpose, cells were cross-linked, chromatin fragmented and ERαS305-P immuno-precipitated. The co-isolated chromatin fragments were amplified, sequenced and mapped against the human genome reference (**Figure 3A**) (35). MCF7 cells were hormone deprived for three days and stimulated with forskolin. Since transcriptional alterations were observed four hours after tamoxifen treatment, the chromatin interaction patterns of ERαS305-P were studied at an earlier time point as DNA binding precedes transcription. ERαS305-P binding patterns were compared to chromatin interactions of total ERα from asynchronously proliferating MCF7 cells (36) to determine the shared events and unique binding sites for the phosphorylated receptor. ERαS305-P shows 3327 binding events, of which 912 overlap with total ERα (**Figure 3C**). The unique subsets of binding patterns were not due to differ-

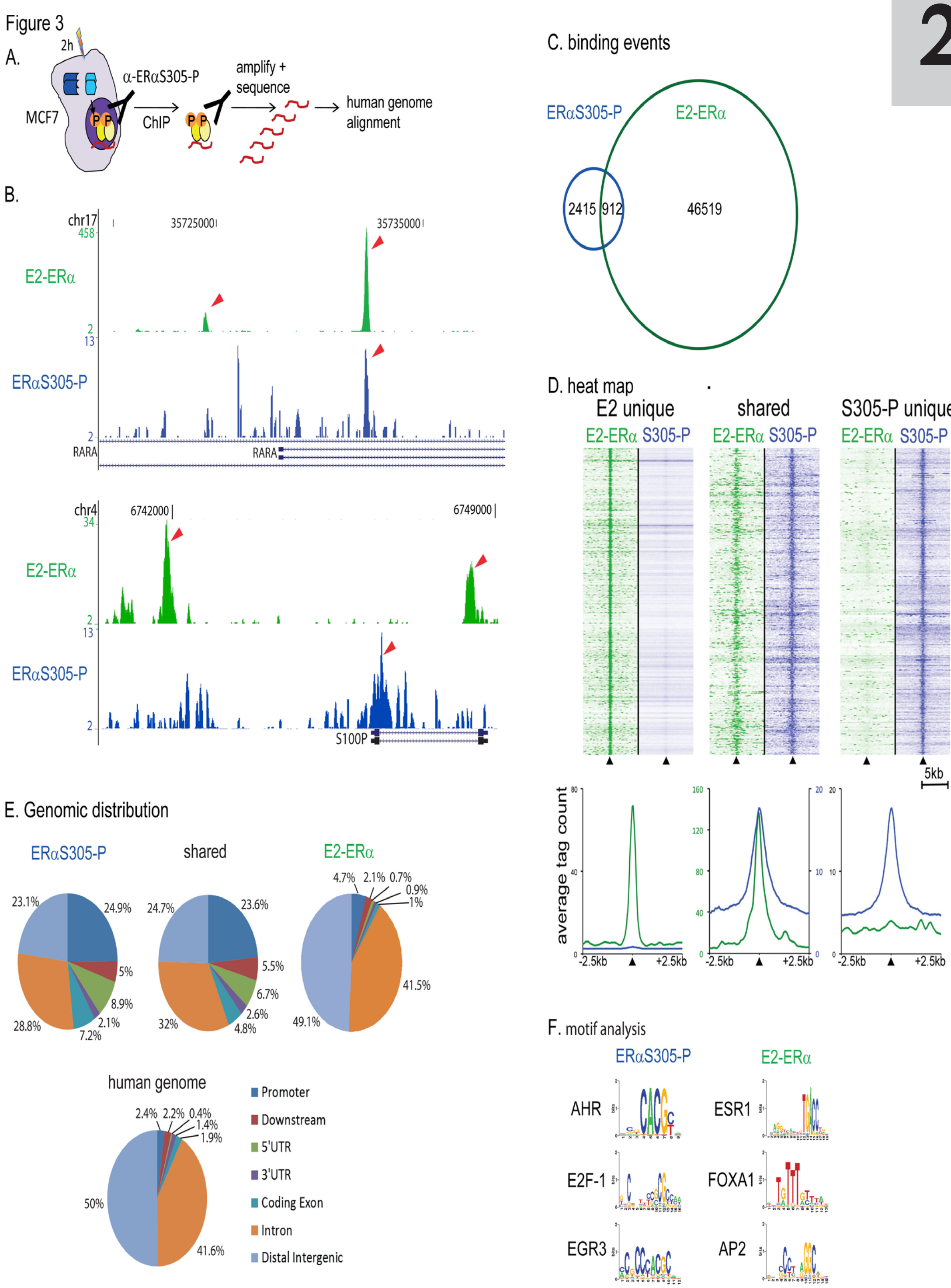

Figure 3
A.
2h
MCF7
α-ERαS305-P
ChIP
amplify + sequence
human genome alignment
B.
chr17
35725000
35735000
E2-ERα
ERαS305-P
RARA
chr4
6742000
6749000
S100P
C. binding events
ERαS305-P
E2-ERα
2415
912
46519
D. heat map
E2 unique
shared
S305-P unique
E2-ERα S305-P
5kb
average tag count
-2.5kb
+2.5kb
E. Genomic distribution
ERαS305-P
shared
E2-ERα
human genome
Promoter
Downstream
5'UTR
3'UTR
Coding Exon
Intron
Distal Intergenic
F. motif analysis
AHR
E2F-1
EGR3
ESR1
FOXA1
AP2

**Figure 3**: *Distinct chromatin binding patterns of ERαS305-P*
*(A) Experimental setup: after 2 hours of forskolin stimulation, ChIPseq is performed using a specific antibody against ERαS305-P. (B) Examples of chromatin interaction to two gene areas for total ERα (green) and S305-phosphorylated ERα (blue). Retinoic acid receptor alpha (RARA) has an ERα binding site within a 20k nucleotide region of the transcription start, to which ERaS305-P also binds. S100P shows binding for both total and phosphorylated ERα, but ERαS305-P prefers the promoter, whereas total ERα binds to a distal enhancer. Arrows denote binding peaks. A 5 kb size marker is indicated. (C) Venn diagram, showing the overlap of ERαS305-P (blue) chromatin binding events versus total ERα (green). Number of shared or unique peaks is indicated. Called peaks were interrogated for overlap and intersected using Galaxy (http://main.g2.bx.psu.edu/). (D) Heat map visualization of the shared and unique peaks for ERαS305-P (blue) and E2-ERα (green). Top: Shown are all peak regions, which were vertically aligned and centered on the binding site (arrowhead) with a 5kb window. Bottom: The signals were quantified and visualized in a 2D line graph, showing the average tag count for ERαS305-P (blue) and total ERα (green) at the shared and unique regions with a 2.5kb window. (E) Genomic distribution of overall ERαS305-P binding (left), total ERα (right) and sites shared between the two (middle). The genomic distributions of binding sites were analyzed using the cis-regulatory element annotation system (CEAS) 57. The genes closest to the binding site on both strands were analyzed. If the binding region is within a gene, CEAS software indicates whether it is in a 5'UTR, a 3'UTR, a coding exon, or an intron. Promoter is defined as 1 kb upstream from RefSeq 5' start. If a binding site is >1 kb away from the RefSeq transcription start site, it is considered distal intergenic. ERαS305-P shows preference for promoter sites. (F) Motif analysis of binding sites for ERαS305-P (blue) and total, estradiol-stimulated ERα (green) show a difference in motif preference. To identify motifs, SeqPos was used 58. SeqPos uses the distances from motif positions to the peak summits (center of the regions) to find the most enriched motifs near peak summits, using TRANSFAC.*

ences in peak-calling thresholds, as shown in the raw heat map distributions (**Figure 3D**). These data imply that S305-phosphorylated ERα shares only a subset of the conventional ERα binding sites, but also has its own specific targets sites. Examples of shared and unique sites are shown in **Figure 3B**. Only a subset of the ERαS305-P binding sites as induced by PKA stimulation are shared with EGF-induced ERα chromatin interactions (**Suppl. Figure S2**) (28). These data suggest that distinct ERα-chromatin interaction patterns are induced through different kinase pathways. When the ERαS305-P peaks were annotated, a striking enrichment for ERαS305-P was observed for promoter regions, 3'UTRs and 5'UTRs, whereas total ERα generally prefers distal enhancers (**Figure 3E**), as described before (37,38). This enrichment on promoter regions is not only observed for the shared interaction sites, but also for unique ERαS305-P peaks. Interestingly, we observed distinct enriched DNA motifs for ERαS305-P as compared to total ERα, implying an active retargeting of the receptor to uncommon sites (**Figure 3F**). The top 3 enriched motifs underlying ERαS305-P binding events were AHR, EGR3 and E2F1. The biological relevance of these transcription factors in tamoxifen resistance was assessed in a cell proliferation assay, which demonstrated that knockdown of AHR, EGR3 and E2F1 can all overcome the growth advantage of PKA-activated MCF7 cells under tamoxifen conditions (**Suppl. Figure S3**). Concluding, modification of ERα at Ser305 not only affects ERα conformation (17), but also chromatin binding sites, transcription and cellular responses.

**Interconnection of genes in the classifier**

To understand how phosphorylation of ERαS305 drives differential gene expression, resulting in tamoxifen unresponsiveness of breast tumors, we decided to define the functional networks that are differentially (in)activated due to S305-phosphorylation of ERα. An Ingenuity Pathway Analysis (IPA) of the differentially regulated genes in both conditions was performed, which identifies functional connections from a gene list using literature data. Within the top pathways listed in **Figure 4A**, classical ERα targets (TFF1, XBP1, CAV1) as well as interacting partners of ERα for non-classical gene transactivation, such as AP-1 and NFκB (**Suppl. Figure S4**) were found, illustrating expected ERα-mediated gene expression rather than only PKA activation. Nonetheless, a pathway analysis comparison between ERαS305-P and estradiol stimulation of ERα resulted in enrichment of distinct molecular pathways (**Suppl. Table S5 and Figure S5**).

As PKA-activation can induce cell growth in tamoxifen-treated breast cancer cells (22,17), we focused on the third network, which links genes in the classifier to cell growth and proliferation. This network includes MYC as a central player (**Figure 4B**). MYC is not a direct hit in our microarray analysis as it was enriched just below the threshold (1.49x) in MCF7 cells. We validated elevated MYC expression in MCF7 cells following forskolin and tamoxifen stimulation by a more quantitative method: qPCR (**Figure 4C**). PKA activation combined with tamoxifen treatment upregulates MYC expression 1.65-fold, directly coupling ERαS305 phosphorylation to expression

Figure 4

| A. | Associated Network Functions | Score |
|---|---|---|
| 1 | Lipid Metabolism, Molecular Transport, Small Molecule Biochemistry | 50 |
| 2 | Cell Signaling, Nucleic Acid Metabolism, Small Molecule Biochemistry | 39 |
| 3 | **Cell Cycle, Cellular Development, Cellular Growth and Proliferation** | 32 |
| 4 | Lipid Metabolism, Small Molecule Biochemistry, Cellular Movement | 24 |
| 5 | Cellular Development, Cellular Growth and Proliferation, Tissue Morphology | 13 |

B.

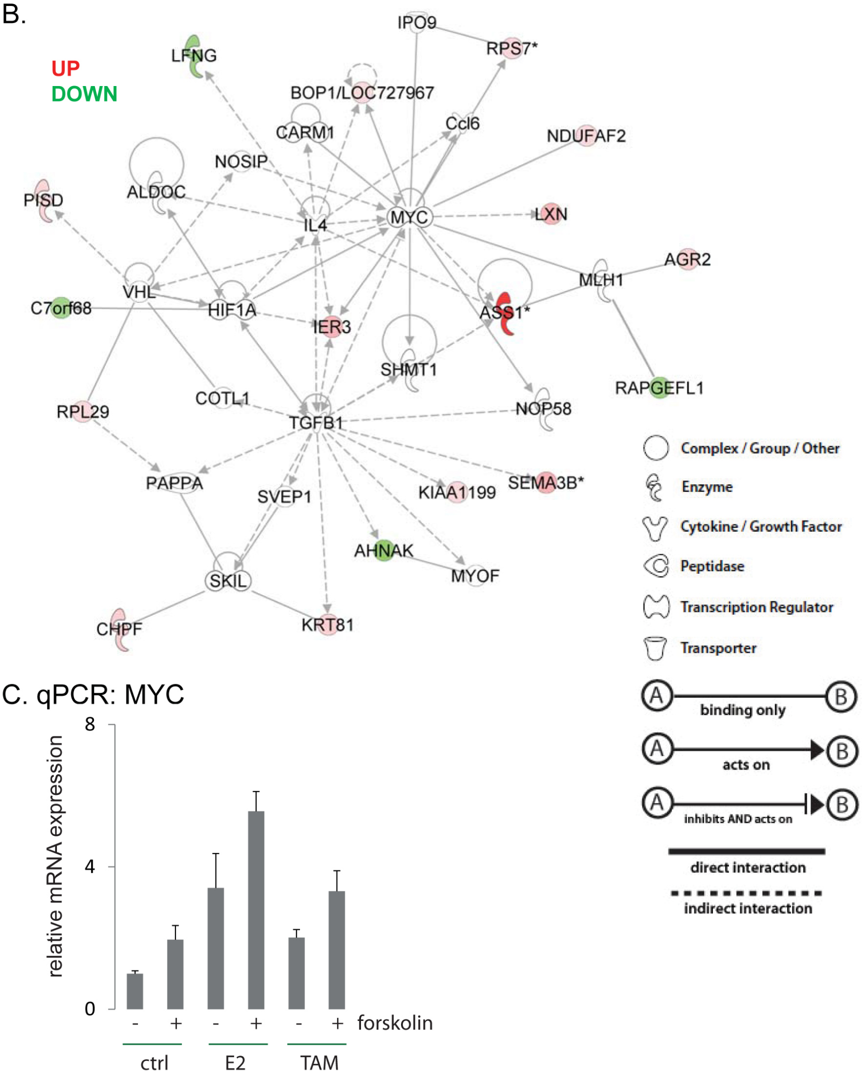

**Figure 4**: *Interconnection of genes in the classifier*
*(A) Ingenuity pathway analyses reveal direct and indirect links between the genes in our classifier, resulting in the top 5 of significant pathway terms listed in the table and shown in Supplementary Figure S4. Networks are scored based on the number of network eligible genes the list contain contains. Score is a likeliness parameter. (B) Shown is network 3 as shown in bold in Figure 4A. MYC plays a key role, targeting several of the genes from the classifier. Differential expression in the microarray in Figure 2 is illustrated by a red (up) or green (down) color. The nature of the different hits is indicated on the right. (C) MYC qPCR of MCF7 cells after 4 hours of treatment with estradiol (E2), tamoxifen (TAM) or hormone depleted (ctrl) in presence or absence of forskolin to stimulate PKA. Error bars represent SEM. * $p < 0.05$ by Student's t-test.*

of a well-known oncogene involved in tamoxifen resistance (39,40). Of note, MYC upregulation is already observed after PKA treatment alone, and no additional treatment with tamoxifen is required.

**Integration of ERαS305-P chromatin binding with gene expression signatures**

Selective ERαS305-P chromatin interactions should translate into transcriptional differences. To assess these, we integrated the ChIP-seq data with the expression data obtained from the microarray studies. This allowed us to extract the direct targets of ERαS305-P from the bulk of genes that are differentially regulated due to overall PKA activation. Among the 100 hits from our classifier, we defined the genes that had a chromatin binding peak for ERαS305-P within a 20k region from the transcription start site, which indicates direct transcriptional regulation by the receptor (41). This identified 26 genes as direct targets of ERαS305-P: 14 of these genes were upregulated and 12 downregulated (**Figure 5A**). Of these direct ERαS305-P targets, nine were distinct from estradiol-stimulated total ERα, implying they are specific for ERαS305-P. Utilized as a classifier in the previously mentioned patient dataset (32), the 26 ERαS305-P targets result in a significant correlation with poor disease outcome (**Figure 5B**. p=0.008 ; HR=2.33). Unfortunately validating the classifier in the *Buffa et al*. (33) dataset was not feasible due to limited patient numbers.

Next, we compared direct ERαS305-P targets with non-phosphorylated ERα with respect to tamoxifen-agonistic response, as measured by qPCR. For non-S305-P target genes, the PKA-stimulatory effects were identical for

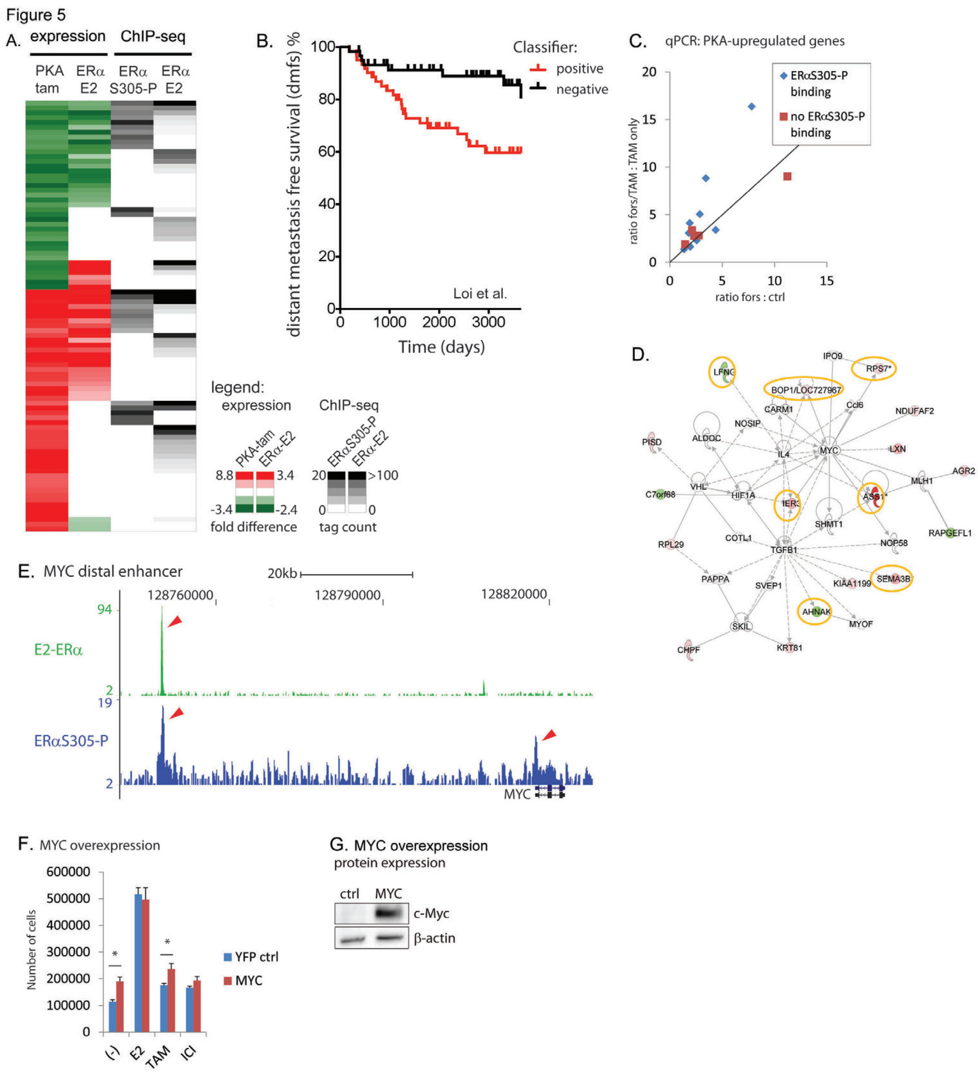


**Figure 5**: *Integration of ERαS305-P chromatin binding and gene expression signatures*

*(A) Hierarchical clustering of the 100 genes in the classifier, based on ERαS305-P chromatin binding, estradiol-induced chromatin interactions and gene expression of total ERα. (B) The 26 ERαS305-P hits were applied as a classifier on the patient dataset derived from Loi et al. (32), resulting in a significant correlation with poor disease outcome (p=0.008 ; HR=2.33 ). Analysis was performed as described in Figure 2D. (C) Scatter plot for qPCR data from genes upregulated by PKA activation, derived from the 100-gene classifier and subdivided into two groups: with (blue*

*diamonds) or without (red squares) a proximal binding site for ERαS305-P. Ratio for PKA activation over no activation is plotted for presence (Y-axis) or absence (X-axis) of tamoxifen. Diagonal line represents equal ratios irrespective of tamoxifen. (D) Six (representing 23%) of the direct targets are found in the MYC-related Ingenuity network, highlighted in orange. (E) ERαS305-P selectively targets MYC by binding to a distal enhancer and the promoter. Shown are the reads for ERα and ERαS305-P around the MYC gene and the 20kb marker. Arrows indicate the two peaks. (F) MYC overexpression enhances tamoxifen-specific MCF7 cell growth. Absolute cell numbers of triplicates are counted and plotted for YFP-control (ctrl in blue) and MYC (in red). Scale bars represent standard deviations. A student T-test was performed; *: p=0.03. (G) c-MYC protein expression analysis of MYC overexpression, compared to control (ctrl) by western blot. Loading control is β-actin*

tamoxifen and vehicle-treated cells implying no tamoxifen-agonism at these genes (**Figure 5C**). However, for the majority of the tested genes with a proximal ERαS305-P binding site, additional transcriptional activity was observed when tamoxifen was combined with PKA treatment, suggesting an agonistic response in addition to PKA stimulation alone (**Figure 5C**).

We then analyzed the new classifier for biological relevance. Seven of the 26 direct targets were functionally connected with MYC, implying that ERαS305-P directly affects the MYC pathway (**Figure 5D**), rather than acting on MYC alone. Since MYC was upregulated in the PKA-activated, tamoxifen-treated MCF7 cells, we explored whether MYC is a direct target of ERαS305-P. To this end, the proximity of the MYC locus was analyzed for ERαS305-P peaks. We observed a chromatin interaction peak at a distal enhancer that has recently been identified (43), and a second peak at the promoter region of MYC (**Figure 5E**, arrows denote the peaks). These and other ERαS305-P/chromatin interaction sites were independently verified by qPCR analysis (**Suppl. Figure S6**). Taken together, we show by ChIP-seq, microarray and qPCR that S305-phosphorylated ERα plays a direct role in MYC transcriptional regulation. MYC upregulation will subsequently affect cell proliferation in response to tamoxifen.

To directly assess the influence of MYC on MCF7 cells proliferation, and the influence of tamoxifen treatment thereon, MYC was transiently overexpressed in MCF7 cells (**Figure 5F**; protein overexpression confirmed in **Figure 5G**). This resulted in a significant increase in cell proliferation both in absence and presence of tamoxifen, linking the enhanced expression of MYC with cell growth even in presence of this anti-estrogen and thus inducing resistance.

**Discussion**

Activation of kinase pathways is one of the hallmarks of tumor formation. Most breast cancers are critically dependent on ERα and this nuclear hormone receptor can be modified by a series of kinases, including PKA (12,13,14,15,17). PKA phosphorylates ERα at position 305, inducing a conformational arrest of the receptor upon tamoxifen exposure (17). This eventually results in tamoxifen resistance and cell proliferation in response to tamoxifen exposure (17,22). However, the exact mechanism of tamoxifen resistance remains unknown and is studied here. We show that S305-P modification has a marked effect on the accurate positioning of ERα on transcriptional start sites. This is highly surprising and, in more general terms, suggests that post-translational modifications can have major effects on chromatin binding of transcription factors and thus the transcriptome. In fact, this couples extracellular signalling (in our case by PKA activation) to alterations in transcriptional output by retargeting ERα to alternative binding regions.

The phosphorylated receptor displayed an enrichment for DNA motifs that were distinct from that of total ERα in proliferating cells, suggesting that the phosphorylation directly alters the DNA binding capacities of specificity of the receptor. The top 3 enriched motifs underlying ERαS305-P binding events were AHR, EGR3 and E2F1. These transcription factors are not surprising hits, since each of these has previously been described to play essential roles in ERα biology. EGR3 has been described to be involved in ERα signalling (44) and ERα-mediated invasion, and its expression correlates with poor outcome (45). E2F1 on the other hand was found to be an ERα target that mediates tamoxifen resistance (46) and estradiol-stimulated cell proliferation (47). AHR crosstalks with ER (43) and modulates ERα-mediated gene regulation (48).

The crystal structure data of the full length RXR:PPARγ heterodimer shows an alignment of the hinge region of PPARγ along the DNA (49). This may also occur with the hinge domain of ERα, thereby determining the DNA motif specificity of the receptor. Any modifications in the hinge domain (including S305 phosphorylation) may, as a consequence, alter the DNA-binding preferences of the receptor. The altered binding repertoire of ERαS305-P is surprising, but unlikely to be dictated by this post-translational modification alone. Most likely, the S305-P modification attracts different co-factors that in assembly alter the chromosome-binding preferences of the receptor. Such effects can be mediated further by phosphorylation of CARM1 (26) or AIB1 (25), but may also be dictated by other factors. ERα binding events are not rigid, but can differ between cell lines (50) and the chromatin-binding pattern can be manipulated by growth factor stimulation (28). To our knowledge, this is the first report describing the direct effect of phosphorylation on the chromatin binding landscape of ERα. The distinct and unique patterns as observed here suggest that phosphorylation events on the receptor not only dictate the transcriptional readout (17), the transcript repertoire (22) and cofactor preferences (21), but also determine to which DNA regions the receptor is able to bind. This yields a complicated view on transcriptional regulation by ERα. As ERα can be modified at different locations by different kinases, different chromatin deposition and thus transcription may be the result. Depending on the activated signalling pathway, a different DNA binding preference of ERα after estrogen activation or tamoxifen exposure may be the result.

Many more ERα/chromatin binding events exist as compared to estradiol-responsive genes (37,51,52). Apparently, the same holds true for ERαS305P binding events. Yet, a clear enrichment of the phosphorylated ERα was found at gene promoters. About 25% of the 3327 binding events was found at a promoter, implying about 830 peaks. Out of the 100 differentially expressed genes that were shared between the MCF7 and MDA-MB134 cell lines, 26 had at least one proximal ERαS305-P binding event, presenting a statistical enrichment over genomic background (Fisher's exact test; $p=0.024$).

Although we find an enrichment at promoters, not all ERαS305-P bound promoters result in the expression of the corresponding gene in our microarray analyses. This could arise due to the temporal nature of the expression array experiments, suggesting different time points may be needed to pick up differential expression of more of these genes. Nevertheless, our data show that an enrichment of ERαS305-P at promoter sites correlates with expression of the corresponding genes.

We show here for the S305 modification that distinct transcriptional pathways are generated that can explain cell growth of breast cancer cells in response to tamoxifen. Ingenuity pathway analysis illustrated that only limited overlap exists between E2 and ERαS305 associated pathways, even though a high-scoring 'cell proliferation' network was shared between the two conditions (Suppl. Figure S5 and Table S5). What the physiological effects from all non-overlapping pathways would be still needs to be deciphered, and the additive value of any of these networks in tamoxifen resistance cannot be ruled out. The ERαS305-P distinct gene set has led to the development of a classifier that allows prediction of patient's responses to tamoxifen treatment. Further analyses show that the MYC pathway in particular can be activated, which may explain the more aggressive behavior of such tumors.

Our data illustrate that one single post-translational modification can have a major impact on the chromatin interaction patterns and transcriptome of the estrogen receptor. ERαS305 phosphorylation greatly alters its DNA-binding repetoire, giving rise to distinct responsive gene signature that includes MYC and its related genes. MYC overexpression overcomes tamoxifen action on cell proliferation and hence, a PKA-induced elevation of MYC would induce resistance to tamoxifen. MYC is a well-described gene target of ERα (40) and not solely an ERαS305P dependent gene. However, here we postulate that MYC activation is a means of PKA-induced tamoxifen-resistance, where the typical E2-dependent MYC gene is now activated by a PKA-induced ERαS305P. A link between tamoxifen resistance and MYC has been previously described (40), for which we now present one mechanism by which this can occur.

The plasticity in the chromatin binding patterns of ERα as induced by PKA activation has significant downstream effects that may lie at the very basis of tamoxifen-resistance of breast cancer patients. The genes differentially targeted and transcribed by S305-phosphorylated ERα indeed act as a biologically relevant and understandable classifier for breast cancer patient responses to tamoxifen treatment.

## Materials and Methods

### Cell culture

MCF7 and MDA-MB134 cells were cultured in DMEM supplemented with 8% FBS and antibiotics (penicillin, streptavidin). To deprive cells of hormones, they were cultured in phenol-red free DMEM with 5% charcoal-treated serum and antibiotics. Cells were stimulated with 10-7 M 4-OH-tamoxifen and/or 10 μM forskolin or vehicle for 4 or 24 hours.

### PKA-RIα knockdown

MDA-MB134 cells were infected with lentivirus containing a shRNA (sequence: GGGGATAACTTCTATGTGA) targeting PKA-RIα. Infection was performed in DMEM after 2h incubation with polybrene (5ug/ml). After infection overnight, DMEM with 8% FBS was refreshed. Selection of infected cells was done with 3ug/ml puromycin.

**Biochemical analysis**
Western blotting was performed according to standard protocols. Antibodies used were anti-ERα (Santa Cruz Biotechnology), anti-ERαS305-P (Millipore/Upstate), anti-β-Actin (Millipore/Chemicon), anti-p-Creb (Cell Signaling Technology), anti-PKA-RIα (BD Transduction Laboratories) and anti-c-MYC (Santa Cruz Biotechnology). Signals were detected with a Lumi-light Plus detection kit (Roche).

**Microarray experiments**
Cells were harvested and homogenized in trizol (Invitrogen). RNA was isolated and hybridized on IlluminaWG-6 expression BeadChip (MDA-MB-134) and Human HT-12 v4 Expression BeadChip (MCF7, performed in triplicate). For data extraction, we used no background correction, applied variance stabilizing transformation and robust spline normalization. Data were log-transformed, ratios of the absolute values were calculated. For the RI plots, the log-ratio was plotted over the intensity, calculated from the absolute intensities as follows: R = log (PKA-activated / control) and I = log (PKA-activated x control). P-values absolute-value ratios were calculated with a two-tailed paired t-test. Hits were selected on $p<0.05$ with a ratio threshold of 1.5x.

**Bioinformatics patient dataset**
We extracted the ERα positive, tamoxifen treated tumors from two published patient datasets (32,33). All the expression data were retrieved for the 100 hits in the classifier. The average expression of all the tested genes was calculated, ranked and divided in two groups. Patients who were stratified in two groups: 1. upregulated genes in the top 50% and the downregulated genes in the bottom 50%. 2. upregulated genes in the bottom 50% and the downregulated genes in the top 50%. Kaplan-Meijer plots were generated using Prism 5 (Graphpad software). P-values were calculated using a log-ranked Gehan-Breslow-Wilcoxon method.

**qPCR**
Cells were harvested and homogenized in trizol. RNA isolation for qPCR was performed by a phenol-chloroform extraction. cDNA was made with a Superscript III RT kit (Invitrogen) using manufacturer's protocols. qPCR for cDNA and for ChIP-DNA was performed with SYBR Green (Applied Bi-

osystems) on a Chromo4 RT detector (Bio-Rad) using standard protocols. Primers (Invitrogen) were designed with primer3 v0.4.0 and are shown in Supplementary table S6.

**ChIP-seq**

ChIP experiments were performed as described previously (53). The antibody used was anti-ERαS305-P (Millipore/Upstate). ChIP DNA was amplified as described (35). Sequences were generated by the Illumina GAIIx genome analyzer (using 36-bp reads), processed by the Illumina analysis pipeline version 1.6.1, and aligned to the Human Reference Genome (assembly hg18, NCBI Build36.1, March 2008) using BWA version 0.5.5. Reads were filtered by removing those with a BWA alignment quality score less than 15. A corresponding set of input sequence reads of similar size was obtained by random sampling from the full set of input sequence reads. Enriched regions of the genome were identified by comparing the ChIP samples to input samples using the MACS peak caller (54) version 1.3.7.1 and SICER version 0.0.1 (55), where only peaks shared by both methods were considered.

**MYC overexpression and cell proliferation assay**

MCF7 cells were cultured in 12-wells plates. After one day of hormone deprivation, MYC was overexpressed by polyethylenimine (PEI, Polysciences (56)) transfection of a RC-CMV c-MYC vector. A pcDNA-YFP empty vector was used as control. Cells were treated in triplicate with estradiol (10-8M), tamoxifen (10-7M), fulvestrant (ICI, 10-7M) or control for 7 days. After trypsinization, cells were counted with a CASYton cell counter (Casy Technology).

**Conflict of Interest**

The authors declare no conflict of interest.

**Acknowledgements**

We thank the Central Microarray Facility of the Netherlands Cancer Institute for processing the microarray samples. RL is in part supported by Top Institute Pharma. WZ is supported by a KWF Dutch Cancer Society Fellowship.

**Author contributions**

RL, JN, RM and WZ designed all the experiments. RL and KF conducted all the experiments, with help from CBT and XA. RL and SC conducted all bioinformatics analyses. The paper was written by RL, JN, KF and WZ, with help from all other authors.

## References

1 Ferlay J, Soerjomataram I, Dikshit R, Eser S, Mathers C, Rebelo M, Parkin DM, Forman D, Bray F. Cancer incidence and mortality worldwide: sources, methods and major patterns in GLOBOCAN 2012. Int J Cancer. 2015; No. 5.

2 Sorlie T, Perou CM, TibshiraniR, Aas T, Geisler S, Johnsen H et al. Gene expression patterns of breast carcinomas distinguish tumor subclasses with clinical implications. Proc Natl Acad Sci U S A 2001; 98: 10869-10874.

3 Shiau AK, BarstadD, Loria PM, Cheng L, Kushner PJ, Agard DA et al. The structural basis of estrogen receptor/coactivator recognition and the antagonism of this interaction by tamoxifen. Cell 1998; 95: 927-937.

4 Robertson JF. Selective oestrogen receptor modulators/new antioestrogens: a clinical perspective. Cancer Treat Rev 2004; 30: 695-706.

5 Holm C, Kok M, Michalides R, Fles R, Koornstra RH, Wesseling J et al. Phosphorylation of the oestrogen receptor alpha at serine 305 and prediction of tamoxifen resistance in breast cancer. J Pathol 2009; 217: 372-379.

6 Kok M, Zwart W, Holm C, Fles R, Hauptmann M, Van't Veer LJ et al. PKA-induced phosphorylation of ERalpha at serine 305 and high PAK1 levels is associated with sensitivity to tamoxifen in ER-positive breast cancer. Breast Cancer Res Treat 2011; 125: 1-12.

7 Bostner J, Skoog, L, Fornander T, Nordenskjold B, and Stal O. Estrogen receptor-alpha phosphorylation at serine 305, nuclear p21-activated kinase 1 expression, and response to tamoxifen in postmenopausal breast cancer. Clin Cancer Res 2010; 16: 1624-1633.

8 Massarweh S, Osborne CK, Creighton CJ, Qin L, Tsimelzon A, Huang S et al. Tamoxifen resistance in breast tumors is driven by growth factor receptor signaling with repression of classic estrogen receptor genomic function. Cancer Res 2008; 68: 826-833.

9 Fan, P., Wang J, Santen RJ, and Yue W. Long-term treatment with tamoxifen facilitates translocation of estrogen receptor alpha out of the nucleus and enhances its interaction with EGFR in MCF-7 breast cancer cells. Cancer Res 2007; 67: 1352-1360.

10 Shou J, Massarweh S, Osborne CK, Wakeling AE, Ali S, Weiss H et al. Mechanisms of tamoxifen resistance: increased estrogen receptor-HER2/neu cross-talk in ER/HER2-positive breast cancer. J Natl Cancer Inst 2004; 96: 926-935.

11 Riggins RB, Schrecengost RS, Guerrero MS, and Bouton AH. Pathways to tamoxifen resistance. Cancer Lett 2007; 256: 1-24.

12 Kirkegaard T, Witton CJ, McGlynn LM, Tovey SM, Dunne B, Lyon A et al. AKT activation predicts outcome in breast cancer patients treated with tamoxifen. J Pathol 2005; 207: 139-146.

13 Gee JM, Robertson JF, Ellis IO, and Nicholson RI. Phosphorylation of ERK1/2 mitogen-activated protein kinase is associated with poor response to anti-hormonal therapy and decreased patient survival in clinical breast cancer. Int J Cancer 2001; 95: 247-254.

14 Kato S, Endoh H, Masuhiro Y, Kitamoto T, Uchiyama S, Sasaki H et al. Activation of the estrogen receptor through phosphorylation by mitogen-activated protein kinase. Science 1995; 270: 1491-1494.

15 Rayala SK, Molli PR, and Kumar R. Nuclear p21-activated kinase 1 in breast cancer packs off tamoxifen sensitivity. Cancer Res 2006; 66: 5985-5988.

16 Rayala SK, Talukder AH, Balasenthil S, Tharakan R, Barnes CJ, Wang RA et al. P21-activated kinase 1 regulation of estrogen receptor-alpha activation involves serine 305 activation linked with serine 118 phosphorylation. Cancer Res 2006; 66: 1694-1701.

17 Michalides R, Griekspoor A, Balkenende A, Verwoerd D, Janssen L, Jalink K et al. Tamoxifen resistance by a conformational arrest of the estrogen receptor alpha after PKA activation in breast cancer. Cancer Cell 2004; 5: 597-605.

18 de Leeuw R, Neefjes J, and Michalides R. A Role for Estrogen Receptor Phosphorylation in the Resistance to Tamoxifen. Int J Breast Cancer 2011.

19 Skliris GP, Rowan BG, Al Dhaheri M, Williams C, Troup S, Begic S et al. Immunohistochemical validation of multiple phospho-specific epitopes for estrogen receptor alpha (ERalpha) in tissue microarrays of ERalpha positive human breast carcinomas. Breast Cancer Res Treat 2009; 118: 443-453.

20 Skliris GP, Nugent ZJ, Rowan BG, Penner CR, Watson PH, and Murphy LC. A phosphorylation code for oestrogen receptor-alpha predicts clinical outcome to endocrine therapy in breast cancer. Endocr Relat Cancer 2010; 17: 589-597.

21 Zwart, W., Griekspoor A, Berno V, Lakeman K, Jalink K, Mancini M et al. PKA-induced resistance to tamoxifen is associated with an altered orientation of ERalpha towards co-activator SRC-1. EMBO J 2007; 26: 3534-3544.

22 Dudek P and Picard D. Genomics of signaling crosstalk of estrogen receptor alpha in breast cancer cells. PLoS One 2008; 3: e1859-.

23 Miller WR. Regulatory subunits of PKA and breast cancer. Ann N Y Acad Sci 2002; 968: 37-48.

24 Wu RC, Qin J, Yi P, Wong J, Tsai SY, Tsai MJ et al. Selective phosphorylations of the SRC-3/AIB1 coactivator integrate genomic reponses to multiple cellular signaling pathways. Mol Cell 2004; 15: 937-949.

25 Yi P, Feng Q, Amazit L, Lonard DM, Tsai SY, Tsai M et al. Atypical protein kinase C regulates dual pathways for degradation of the oncogenic coactivator SRC-3/AIB1. Mol Cell 2008; 29: 465-476.

26 Carascossa S, Dudek P, Cenni B, Briand PA, and Picard D. CARM1 mediates the ligand-independent and tamoxifen-resistant activation of the estrogen receptor alpha by

cAMP. Genes Dev 2010; 24: 708-719.
27 Lupien M, Eeckhoute J, Meyer CA, Krum SA, Rhodes DR, Liu XS et al. Coactivator function defines the active estrogen receptor alpha cistrome. Mol Cell Biol 2009; 29: 3413-3423.
28 Lupien M, Meyer CA, Bailey ST, Eeckhoute J, Cook J, Westerling T et al. Growth factor stimulation induces a distinct ER(alpha) cistrome underlying breast cancer endocrine resistance. Genes Dev 2010; 24: 2219-2227.
29 Reiner GC and Katzenellenbogen BS. Characterization of estrogen and progesterone receptors and the dissociated regulation of growth and progesterone receptor stimulation by estrogen in MDA-MB-134 human breast cancer cells. Cancer Res 1986; 46: 1124-1131.
30 Al Dhaheri MH and Rowan BG. Protein Kinase A Exhibits Selective Modulation of Estradiol-Dependent Transcription in Breast Cancer Cells that Is Associated with Decreased Ligand Binding, Altered Estrogen Receptor {alpha} Promoter Interaction, and Changes in Receptor Phosphorylation. Mol Endocrinol 2007; 21: 439-456.
31 Bossis I and Stratakis CA. Minireview: PRKAR1A: normal and abnormal functions. Endocrinology 2004; 145: 5452-5458.
32 Loi S, Haibe-Kains B, Desmedt C, Lallemand F, Tutt AM, Gillet C et al. Definition of clinically distinct molecular subtypes in estrogen receptor-positive breast carcinomas through genomic grade. J Clin Oncol 2007; 25: 1239-1246.
33 Buffa FM, Camps C, Winchester L, Snell CE, Gee HE, Sheldon H et al. microRNA-Associated Progression Pathways and Potential Therapeutic Targets Identified by Integrated mRNA and microRNA Expression Profiling in Breast Cancer. Cancer Res 2011; 71: 5635-5645.
34 Chen D, Pace PE, Coombes RC, and Ali S. Phosphorylation of human estrogen receptor alpha by protein kinase A regulates dimerization. Mol Cell Biol 1999; 19: 1002-1015.
35 Schmidt D, Wilson MD, Spyrou C, Brown GD, Hadfield J, and Odom DT. ChIP-seq: using high-throughput sequencing to discover protein-DNA interactions. Methods 2009; 48: 240-248.
36 Robinson JL, Macarthur S, Ross-Innes CS, Tilley WD, Neal DE, Mills IG et al. Androgen receptor driven transcription in molecular apocrine breast cancer is mediated by FoxA1. EMBO J 2011; 30: 3019-3027.
37 Carroll JS, Meyer CA, Song J, Li W, Geistlinger TR, Eeckhoute J et al. Genome-wide analysis of estrogen receptor binding sites. Nat Genet 2006; 38: 1289-1297.
38 Madak-Erdogan Z, Lupien M, Stossi F, Brown M, and Katzenellenbogen BS. Genomic collaboration of estrogen receptor alpha and extracellular signal-regulated kinase 2 in regulating gene and proliferation programs. Mol Cell Biol 2011; 31: 226-236.
39 Miller TW, Balko JM, Ghazoui Z, Dunbier A, Anderson H, Dowsett M et al. A gene expression signature from human breast cancer cells with acquired hormone independence

identifies MYC as a mediator of antiestrogen resistance. Clin Cancer Res 2011; 17: 2024-2034.

40 Musgrove EA, Sergio CM, Loi S, Inman CK, Anderson LR, Alles MC et al. Identification of functional networks of estrogen- and c-Myc-responsive genes and their relationship to response to tamoxifen therapy in breast cancer. PLoS One 2008; 3: e2987-.

41 Louie MC, McClellan A, Siewit C, Kawabata L. Estrogen receptor regulates E2F1 expression to mediate tamoxifen resistance. Mol Cancer Res 2010; 8: 343-352.

42 Fullwood MJ, Liu MH, Pan YF, Liu J, Xu H, Mohamed YB et al. An oestrogen-receptor-alpha-bound human chromatin interactome. Nature 2009; 462: 58-64.

43 Wang C, Mayer JA, Mazumdar A, Fertuck K, Kim H, Brown M et al. Estrogen Induces c-myc Gene Expression via an Upstream Enhancer Activated by the Estrogen Receptor and the AP-1 Transcription Factor. Mol Endocrinol 2011; 25: 1527-1538.

44 Inoue A, Omoto Y, Yamaguchi Y, Kiyama R, Hayashi SI. Transcription factor EGR3 is involved in estrogen-signaling pathway in breast cancer cells. J Mol Endocrinol 2004; 32: 649-661.

45 Suzuki T, Inoue A, Miki Y, Moriya T, Akahira J, Ishida T et al. Early growth responsive gene 3 in human breast carcinoma: a regulator of estrogen-meditated invasion and a potent prognostic factor. Encocr Relat Cancer 2007; 14: 279-292

46 Frietze S, Lupien M, Silver PA, Brown M. CARM1 regulates estrogen-stimulated breast cancer growth through up-regulation of E2F1. Cancer Res 2008; 68: 301-306.

47 Callero MA, Loaiza-Pérez AI. The role of aryl hydrocarbon receptor and crosstalk with estrogen receptor in response of breast cancer cells to the novel antitumor agents benzothiazoles and aminoflavone. Int J Breast Cancer 2011; 923250.

48 Madak-Erdogan Z and Katzenellenbogen BS. Aryl hydrocarbon receptor modulation of estroge receptor a-mediated gene regulation by a multimeric chromatin complex involving the two receptors and the coregulator RIP140. Toxicol Sci 2012; 125: 401-411.

49 Chandra V, Huang P, Hamuro Y, Raghuram S, Wang Y, Burris TP et al. Structure of the intact PPAR-gamma-RXR-alpha nuclear receptor complex on DNA. Nature 2008; 350-356.

50 Krum SA, Miranda-Carboni GA, Lupien M, Eeckhoute J, Carroll JS, and Brown M. Unique ERalpha cistromes control cell type-specific gene regulation. Mol Endocrinol 2008; 22: 2393-2406.

51 Welboren WJ, van Driel MA, Janssen-Megens EM, van Heeringen SJ, Sweep FC, Span PN et al. ChIP-Seq of ERalpha and RNA polymerase II defines genes differentially responding to ligands. EMBO J 2009; 28: 1418-1428.

52 Hurtado A, Holmes KA, Ross-Innes CS, Schmidt D, Carroll JS. FOXA1 is a key determinant of estrogen receptor function and endocrine response. Nat Genet 2009; 43: 27-33.

53 Carroll JS, Liu XS, Brodsky AS, Li W, Meyer CA, Szary AJ et al. Chromosome-wide mapping of estrogen receptor binding reveals long-range regulation requiring the forkhead protein FoxA1. Cell 2005; 15: 33-43.
54 Zhang Y, Liu T, Meyer CA, Eeckhoute J, Johnson DS, Bernstein, B. E. et al. Model-based analysis of ChIP-Seq (MACS). Genome Biol 2008; 9: R137-.
55 Zang C, Schones DE, Zeng C, Cui K, Zhao K, Peng W. A clustering approach for identification of enriched domains from histone modification ChIP-Seq data. Bioinformatics 2009; 25: 1952-8.
56 Boussif O, Lezoualc'h F, Zanta MA, Mergny MD, Scherman D, Demeneix B et al. A versatile vector for gene and oligonucleotide transfer into cells in culture and in vivo: polyethylenimine. Proc Natl Acad Sci U S A 1995; 92: 7297-7301.
57 Ji X, Li W, Song J, Wei L, and Liu XS. CEAS: cis-regulatory element annotation system. Nucleic Acids Res 2006; 34: W551-W554.
58 He HH, Meyer CA, Shin H, Bailey ST, Wei G, Wang Q et al. Nucleosome dynamics define transcriptional enhancers. Nat Genet 2010; 42: 343-347.

**Supplementary information**

**Supplementary Figure S1**: *Western blot analysis in MCF7 and MDA-MB134 cells, in which PKA was activation by forskolin and/or PKA-RIγ knockdown. In each condition and cell line, ERαS305 phosphorylation could be induced.*

**Supplementary Figure S2**: *Venn diagram, showing shared and unique binding events for E2-ERα, EGF-stimulated ERα (green; Lupien et al., Genes Dev 2010 Oct 1;24(19):2219-27.) and ERαS305-P (blue).*

**Supplementary Figure S3**: *Cell proliferation assay after knockdown of the transcription factors AHR, E2F-1, EGR or ESR1. Cells were seeded in a 384 wells plate and transfected with a smartpool of 4 siRNAs, targeting the corresponding transcription factor using standard protocols (Dharmacon). Cell proliferation was assessed with an Incucyte device (Essen Bioscience) using standard settings. Bars show SD from 4 replicate samples and well confluence at the onset of the experiment was set at 1. Knockdown of these transcription factors can overcome the growth advantage of PKA-activated MCF7 cells under tamoxifen conditions, compared to control.*

**Supplementary Figure S4**: *Ingenuity pathway analysis (IPA), illustrating the networks 1,2,4 and 5 as described in Figure 3A.*

**Supplementary Figure S5**: *Venn diagram, corresponding with Ingenuity Pathway analysis presented in Suppl. Table S5. Image shows the number of enriched networks for overlapping and distinct pathways in PKA-induced ERαS305-P versus estradiol-stimulated ERα in MCF7 cells.*

**Supplementary Figure S6**: *ChIP-qPCR validation. MCF7 were hormone-deprived for 3* *days prior to onset of the experiment. PKA was stimulated using forskolin and ChIP was performed using an ERαS305-P antibody, identical to what was performed for the ChIP-seq. Enrichment of isolated chromatin fragments was assessed by qPCR, which was normalized over control and input.*

**Supplementary Table 1***: Gene expression profile for PKA-activation in MCF7. Genes are ranked from strongest down- to strongest upregulated gene, indicated by the ratio, or fold-difference, of PKA-activated over non-activated cells in presence of tamoxifen.*

**Supplementary Table 2***: Gene expression profile for PKA-activation in MDA-MB134. Genes are ranked from strongest down- to strongest upregulated gene, indicated by the ratio, or fold-difference, of PKA-activated over non-activated cells in presence of tamoxifen.*

**Supplementary Table 3***: Upregulated genes shared between MCF7 and MDA-MB134 (1st part of the 100-gene classifier). Upregulated genes from the microarray profiles presented in Suppl. Tables 1 and 2 were compared, resulting in 59 overlapping genes as presented in a Venn diagram (Figure 2B top).*

**Supplementary Table 4***: Downregulated genes shared between MCF7 and MDA-MB134 (2nd part of the 100-gene classifier) Downregulated genes from the microarray profiles presented in Suppl. Tables 1 and 2 were compared, resulting in 41 overlapping genes as presented in a Venn diagram (Figure 2B bottom).*

**Supplementary Table 5***: Ingenuity Pathway analyses show enriched networks for overlapping genes and distinct gene sets in PKA-induced ERαS305-P and estradiol-stimulated ERα in MCF7 cells.*

**Supplementary Table 6***: qPCR primers for hit validation on mRNA (top) and ChIP (bottom) samples, designed with primer3 v0.4.0.*

Supplementary Figure S1 – Western blot analysis of PKA activation by forskolin treatment and PKA-RIα knockdown in MCF7 and MDA-MB134 cells

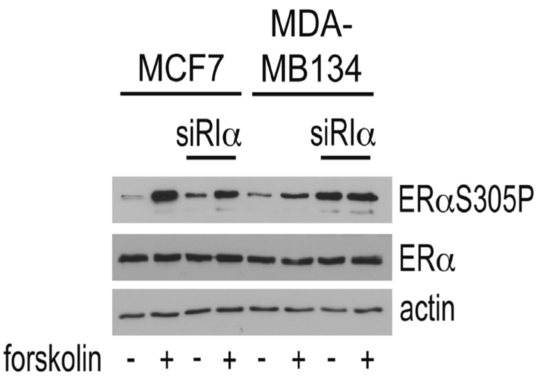


Supplementary Figure S2 – Venn diagram of ERαS305-P ChIPseq data compared with ERα-E2 and ERα-EGF data


Supplementary Figure S3 – Growth assay after knockdown of AHR, E2F-1, EGR or ESR1

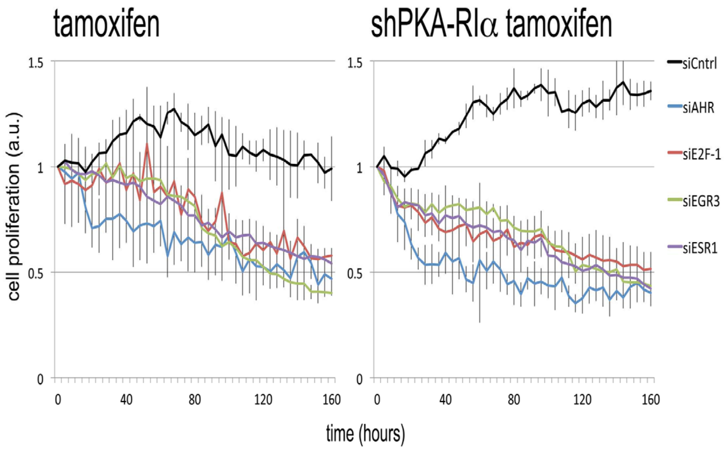

Supplementary figure S4

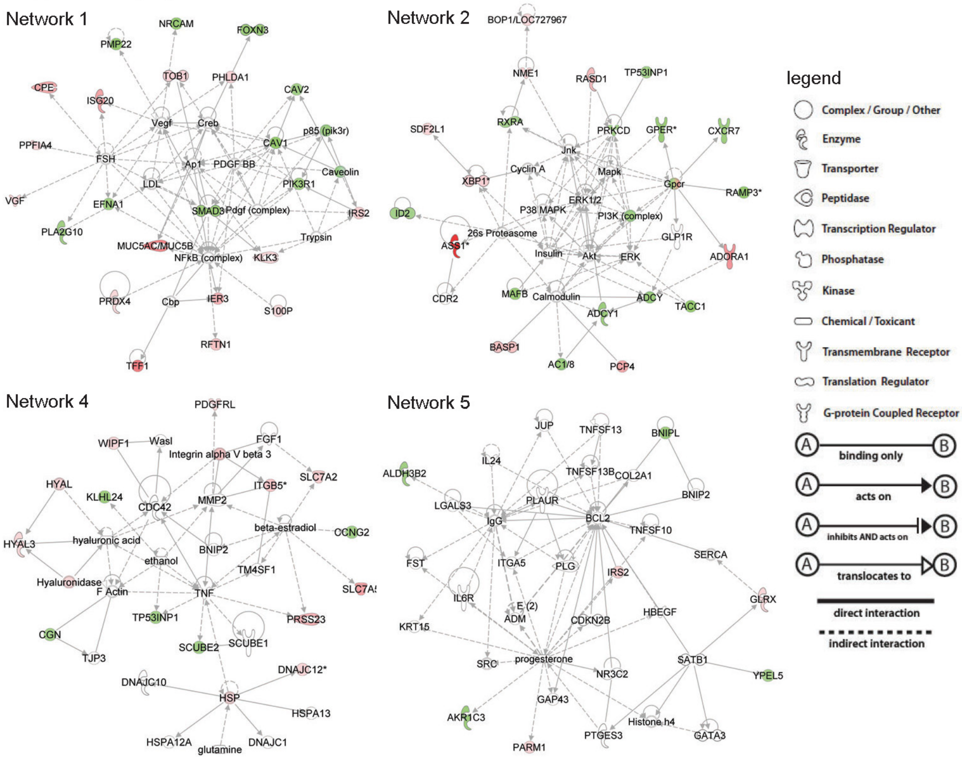


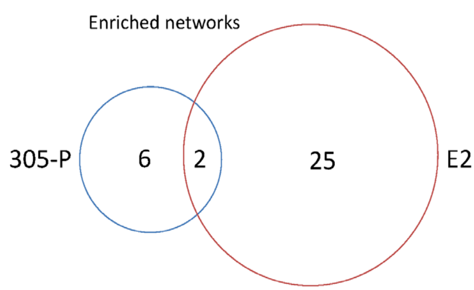


Supplementary Figure S5 – Venn diagram of Ingenuity Pathway analysis of ERαS305-P only, E2 only and overlapping gene sets (See Suppl. Table 5)

Supplementary Figure S6:qPCR validation of ERαS305-P ChIP-seq

| primer set | fold enrichment/ control | related to Figure/Table |
|---|---|---|
| **myc enhancer** | 273 | Fig 5E |
| **myc promoter** | 23 | Fig 5E |
| **S100P promoter** | 241 | Fig 3B |
| **XBP1 enhancer** | 279 | Fig 5A |
| **IER3 promoter** | 31 | Fig 5A |
| **SEMA3B promoter** | 32 | Fig 5A |

**Supplementary Table 1**: *Gene expression profile for PKA-activation in MCF7.*
*See online supplemental information*
**Supplementary Table 2**: *Gene expression profile for PKA-activation in MDA-MB134.*
*See online supplemental information*

**Supplementary Table 3**: *Upregulated genes shared between MCF7 and MDA-MB134 (1st part of the 100-gene classifier).*

| | Symbol | Accession | MCF7 | MDA-MB134 |
|---|---|---|---|---|
| 1 | ASS1\|ASS | NM_000050.4\|NM_000050.3 | 8,758 | 3,471 |
| 2 | ASS | NM_054012.2 | 7,646 | 3,163 |
| 3 | TFF1 | NM_003225.2 | 5,373 | 12,485 |
| 4 | MUC5AC | XM_001134429.1\|XM_495860.2 | 5,106 | 2,694 |
| 5 | ADORA1 | NM_000674.1 | 4,362 | 5,006 |
| 6 | SLC7A5 | NM_003486.5 | 3,886 | 4,248 |
| 7 | ISG20 | NM_002201.4 | 3,703 | 1,921 |
| 8 | CPE | NM_001873.1 | 3,557 | 16,949 |
| 9 | PCP4 | NM_006198.2 | 3,542 | 1,863 |
| 10 | SEMA3B | NM_001005914.1 | 3,224 | 3,122 |
| 11 | IER3 | NM_003897.3\|NM_052815.1 | 3,091 | 3,769 |
| 12 | PRSS23 | NM_007173.4\|NM_007173.3 | 3,071 | 4,128 |
| 13 | LXN | NM_020169.2 | 2,991 | 1,710 |
| 14 | RASD1 | NM_016084.3 | 2,756 | 1,820 |
| 15 | BASP1 | NM_006317.3 | 2,441 | 2,726 |
| 16 | FAM46A | NM_017633.2\|NM_017633.1 | 2,440 | 1,907 |
| 17 | RFTN1\|RA | NM_015150.1 | 2,408 | 1,690 |
| 18 | ITGB5 | NM_002213.3 | 2,318 | 1,659 |
| 19 | CHPF | NM_024536.4 | 2,073 | 1,650 |
| 20 | SLC7A2 | NM_001008539.2\|NM_003046.2 | 1,984 | 3,880 |
| 21 | IRS2 | NM_003749.2 | 1,962 | 1,528 |
| 22 | ITGB5 | NM_002213.3\|XM_944693.1 | 1,953 | 1,544 |
| 23 | AGR2 | NM_006408.2 | 1,907 | 2,017 |
| 24 | KRT81\|KR | NM_002281.2 | 1,897 | 2,354 |
| 25 | XBP1 | NM_005080.2 | 1,847 | 1,763 |
| 26 | SEMA3B | NM_001005914.1 | 1,838 | 1,806 |
| 27 | XBP1 | NM_001079539.1 | 1,795 | 1,674 |
| 28 | HS.579631 | BU536065 | 1,787 | 2,898 |
| 29 | RPS7 | NM_001011.3 | 1,762 | 1,551 |
| 30 | PHLDA1 | NM_007350.3\|NM_007350.2 | 1,762 | 2,174 |
| 31 | MAOA | NM_000240.2 | 1,761 | 1,730 |
| 32 | VGF | NM_003378.2 | 1,745 | 1,574 |
| 33 | TOB1 | NM_005749.2 | 1,740 | 2,895 |
| 34 | NME1 | NM_000269.2\|NM_198175.1 | 1,735 | 2,040 |
| 35 | PISD | NM_014338.3 | 1,706 | 2,757 |
| 36 | SDF2L1 | NM_022044.2 | 1,703 | 1,803 |
| 37 | RPS7 | NM_001011.3 | 1,702 | 1,535 |
| 38 | DKFZP564 | NM_015393.2 | 1,694 | 2,685 |
| 39 | DNAJC12 | NM_021800.2 | 1,694 | 1,703 |
| 40 | PPFIA4 | NM_015053.1 | 1,692 | 1,514 |
| 41 | NUCB2 | NM_005013.2\|NM_005013.1 | 1,681 | 1,528 |
| 42 | PDGFRL | NM_006207.1 | 1,680 | 1,873 |
| 43 | DNAJC12 | NM_021800.2 | 1,663 | 1,574 |
| 44 | SLC47A1\|F | NM_018242.2 | 1,661 | 1,525 |
| 45 | HYAL3 | NM_003549.2 | 1,659 | 1,512 |
| 46 | GLRX | NM_002064.1 | 1,657 | 2,063 |
| 47 | KIAA1324 | NM_020775.2 | 1,652 | 2,827 |
| 48 | WIPF1 | NM_001077269.1 | 1,635 | 1,533 |
| 49 | DNAJC12 | NM_201262.1 | 1,609 | 1,972 |
| 50 | KIAA1199 | NM_018689.1 | 1,606 | 2,496 |
| 51 | KLK3 | NM_001030050.1 | 1,595 | 2,449 |
| 52 | RPL29 | NM_000992.2 | 1,565 | 1,748 |
| 53 | S100P | NM_005980.2 | 1,560 | 1,839 |
| 54 | NDUFA12L | NM_174889.3\|NM_174889.2 | 1,558 | 2,043 |
| 55 | RGS22 | NM_015668.2 | 1,551 | 2,565 |
| 56 | PRDX4 | NM_006406.1 | 1,550 | 1,952 |
| 57 | HS.543887 | CD640673 | 1,548 | 2,079 |
| 58 | FAM108C1 | NM_021214.1\|XM_051862.7 | 1,546 | 1,936 |
| 59 | BOP1 | NM_015201.3 | 1,516 | 1,816 |

**Supplementary Table 4**: *Downregulated genes shared between MCF7 and MDA-MB134 (2nd part of the 100-gene classifier).*

| | Symbol | Accession | MCF7 | MDA-MB134 |
|---|---|---|---|---|
| 1 | CLIC3 | NM_004669.2 | 0,293 | 0,455 |
| 2 | AHNAK | NM_001620.1 | 0,499 | 0,643 |
| 3 | CAV1 | NM_001753.3 | 0,508 | 0,264 |
| 4 | TACC1 | NM_006283.1 | 0,514 | 0,496 |
| 5 | PMP22 | NM_153321.1\|NM_153322.1 | 0,522 | 0,579 |
| 6 | RAMP3 | NM_005856.2 | 0,524 | 0,634 |
| 7 | YPEL3 | NM_031477.4\|NM_031477.3 | 0,531 | 0,664 |
| 8 | NRCAM | NM_005010.3 | 0,546 | 0,622 |
| 9 | GPER\|GPI | NM_001039966.1\|NM_001031682.1 | 0,551 | 0,637 |
| 10 | SMAD3 | NM_005902.3 | 0,554 | 0,474 |
| 11 | MAFB | NM_005461.3 | 0,555 | 0,517 |
| 12 | CHES1 | NM_005197.2 | 0,558 | 0,619 |
| 13 | AKR1C3 | NM_003739.4 | 0,561 | 0,520 |
| 14 | ADCY1 | NM_021116.1 | 0,567 | 0,651 |
| 15 | RAMP3 | NM_005856.1\|NM_005856.2 | 0,571 | 0,594 |
| 16 | CXCR7\|CI | NM_020311.2\|NM_020311.1 | 0,578 | 0,459 |
| 17 | GPER\|GPI | NM_001039966.1 | 0,579 | 0,552 |
| 18 | RAPGEFL | NM_016339.2\|NM_016339.1 | 0,579 | 0,654 |
| 19 | LFNG | NM_001040167.1\|NM_002304.1 | 0,579 | 0,658 |
| 20 | C6orf141 | NM_153344.1 | 0,584 | 0,632 |
| 21 | BNIPL | NM_138278.2\|NM_138278.1 | 0,584 | 0,613 |
| 22 | KLHL24 | NM_017644.3 | 0,589 | 0,453 |
| 23 | TSPAN9 | NM_006675.3 | 0,594 | 0,495 |
| 24 | ALDH3B2 | NM_001031615.1\|NM_000695.3 | 0,594 | 0,538 |
| 25 | PIK3R1 | NM_181523.1\|NM_181504.2 | 0,594 | 0,646 |
| 26 | EFNA1 | NM_004428.2 | 0,597 | 0,601 |
| 27 | PLA2G10 | NM_003561.1 | 0,601 | 0,583 |
| 28 | YPEL2 | NM_001005404.3 | 0,608 | 0,633 |
| 29 | LOC64281 | XR_018564.1\|XM_926703.1 | 0,616 | 0,631 |
| 30 | PRKCD | NM_006254.3\|NM_212539.1 | 0,616 | 0,557 |
| 31 | CCNG2 | NM_004354.1 | 0,629 | 0,661 |
| 32 | SCUBE2 | NM_020974.1 | 0,632 | 0,465 |
| 33 | TP53INP1 | NM_033285.2 | 0,638 | 0,544 |
| 34 | CAV2 | NM_001233.3 | 0,638 | 0,427 |
| 35 | LMTK3 | XM_936372.2\|XM_936372.1 | 0,639 | 0,531 |
| 36 | HIG2 | NM_013332.3\|NM_013332.1 | 0,640 | 0,578 |
| 37 | CGN | NM_020770.1 | 0,648 | 0,641 |
| 38 | ID2 | NM_002166.4 | 0,650 | 0,593 |
| 39 | RXRA | NM_002957.3 | 0,658 | 0,635 |
| 40 | YPEL5 | NM_016061.1 | 0,659 | 0,562 |
| 41 | SAMD11 | NM_152486.2 | 0,664 | 0,446 |

**Supplementary Table 5**: *Ingenuity Pathway analyses.*

*See online supplemental information*

**Supplementary Table 6**: *qPCR primers for hit validation on mRNA (top) and ChIP (bottom) samples.*

*See online supplemental information*